IOP Publishing Journal of Physics: Condensed Matter
J. Phys.: Condens. Matter **32** (2020) 155802 (10pp) https://doi.org/10.1088/1361-648X/ab62be

Disorder-driven non-Fermi liquid behavior in itinerant ferromagnet α-Co_5Ge_3

Meng Song[1,2], Cong Xian[1,2], Yihao Wang[1,2], Jiangpeng Song[1,2], Zhihao Li[1], Langsheng Ling[1], Lei Zhang[1], Yuyan Han[1], Liang Cao[1] and Yimin Xiong[1,3]

[1] Anhui Province Key Laboratory of Condensed Matter Physics at Extreme Conditions, High Magnetic Field Laboratory of the Chinese Academy of Sciences, Hefei, Anhui 230031, People's Republic of China
[2] University of Science and Technology of China, Hefei, Anhui 230026, People's Republic of China
[3] Collaborative Innovation Center of Advanced Microstructures, Nanjing, 210093, People's Republic of China

E-mail: yyhan@hm.ac.cn, lcao@hmfl.ac.cn and yxiong@hmfl.ac.cn

Received 15 October 2019, revised 24 November 2019
Accepted for publication 17 December 2019
Published 10 January 2020

Abstract

The physical properties of itinerant ferromagnet α-Co_5Ge_3 with both strong disorder and spin fluctuations was studied. The dc and ac susceptibility show that both spin fluctuations and disorder dominate the physical properties. In the spin glass phase, with a coexisting ferromagnetic state ($\leqslant$30 K), both non-Fermi liquid behavior and large exponent of scaling relation of $\rho_{xy}^{A} \propto \rho_{xx}^{6.9}$ are observed and attributed to the spin fluctuations and disorder induced by cobalt defects. Upon the increase of external field, Fermi liquid behavior restores due to the suppression of spin fluctuations and disorder. In addition, a large anomalous Hall coefficient R_s is observed. Our results suggest that α-Co_5Ge_3 is a typical itinerant ferromagnet to explore the interplay of disorder and spin fluctuations.

Keywords: non-Fermi liquid behavior, spin fluctuation, disorder, itinerant ferromagnet, anomalous Hall effect

S Supplementary material for this article is available online

(Some figures may appear in colour only in the online journal)

1. Introduction

Breakdown of Landau Fermi liquid (FL) theory is an important topic in the experimental and theoretical investigations of correlated electronic systems [1–5]. Non-Fermi liquid (NFL) behavior has been widely observed in several categories of strongly correlated metals, including heavy fermion (HF) metals [1, 2, 4, 6, 7], high temperature superconductors [3, 8–11], low dimensional compounds [12–14] and itinerant magnets (IMs) [2–4, 15–17]. These NFL systems show unusual temperature dependence in their physical properties at low temperature, including anomalous temperature dependence of resistivity, diverging specific heat coefficient and anomalous Curie–Weiss law of susceptibility. These anomalous properties over wide temperature ranges have attracted continuous interest of theoretical studies [2–5], and also have played an important role in interpreting experimental efforts. Among these theories, the self-consistent renormalization (SCR) theory of spin fluctuations [3, 5, 18–20] worked impressively well for the IMs with *d*-electron [2] or non-magnetic elements [15, 21]. For instance, in itinerant ferromagnetic metals (IFMs) Ni_3Al, YNi_3, $ZrZn_2$ and $(Sc_{1-x}Lu_x)_{3.1}In$, NFL behavior ascribing to spin fluctuations was observed over broad ranges under pressure, temperature, and doping [15, 17, 21, 22], coexisting with long range ferromagnetic (FM) order.

In many NFL systems, rising evidence is revealing that the anomalous behaviors could arise from the disorder induced by doping, allotropic magnetic phase, polycrystalline phase or frustration. Although the effects of disorder have been studied extensively [3, 15, 23–33], exploring the effect of disorder is still one of the challenges in condensed matter physics because disorder appears naturally from the experimental

point of view. Whereas, the SCR theory of spin fluctuations does not include any type of microscopic disorder, therefore the effect of disorder and its interplay with spin fluctuations in IFMs with NFL behavior are still open questions [2, 3, 25, 34]. On the other hand, it is fascinating that the strong disorder can dominate the physics and lead to exotic states of matter, such as spin glass phase which is considered to be the origin of NFL behavior of heavy fermion alloys [2, 3]. This is also important for the completion of theoretical picture of NFL behavior [35]. As a consequence, it will be alluring to investigate the properties of spin glass phase in IFM compounds.

Transition-metal germanide Co_5Ge_3 with magnetic cobalt triangular lattices has two identified phases: low temperature phase of α-Co_5Ge_3 with orthorhombic Co_2Si-type structure (space group *Pnma*) (as shown in figure 1(a)) and high temperature phase of β-Co_5Ge_3 with hexagonal Ni_2in-type structure (space group $P6_3/mmc$) [36–38]. Both α-Co_5Ge_3 and β-Co_5Ge_3 are FM materials with Curie temperatures of 46.4 K and 4 K, respectively [38]. In α-Co_5Ge_3, cobalt triangular lattices form a quasi-two-dimensional network in *ac* plane, as seen in figure 1(b). However, geometrical frustrations are absent as cobalt triangular lattices are non-regular. It is thus expected that the spin fluctuations are significant subject to experimental results. Meanwhile, the defects induced by the nonstoichiometry of cobalt, serving as intrinsic disorder in both lattice and spin structure, are expected to plays an important role on physical properties as well. All these features make α-Co_5Ge_3 a promising candidate to investigate the interplay of spin fluctuations and disorder in IFM materials.

In this work, we investigate the magnetic and transport properties of IFM α-Co_5Ge_3. At low temperature($\leqslant$30 K), a spin glass phase is observed, coexisting with FM state. A NFL behavior is revealed by temperature dependence of resistivity in this phase, which arises from both spin fluctuations and disorder. In α-Co_5Ge_3, disorder plays a more important role than spin fluctuations. An unconventional anomalous Hall scaling relation of $\rho_{xy}^{A} \propto \rho_{xx}^{6.9}$ is observed in the same temperature range, attributing to the strong disorder induced by cobalt defects. Our results demonstrate that, in IFM systems, both spin fluctuations and strong disorder can induce novel properties of the NFL behavior and unconventional anomalous Hall effect.

2. Experimental details

High-quality α-Co_5Ge_3 single crystals were synthesized by the chemical vapor transport (CVT) method by using iodine (I_2) as the transport agent. Single crystal x-ray diffraction (XRD) was measured at room temperature by using a diffractometer Rigaku-TTR3 with Cu K_α to determine crystal orientation. The energy-dispersive x-ray spectroscopy (EDX) was employed to analyze the chemical composition of single crystals on Oxford SWIFT3000 spectroscopy. The transport measurements were performed on Oxford Instrument TeslatronPT cryogenic system and quantum design physical property measurement system (PPMS) by dc four-probe method. The magnetic measurements were carried out on quantum design 7 T Magnetic Property Measurement System (MPMS3).

3. Results and discussion

The crystal structure of α-Co_5Ge_3 is depicted in figures 1(a) and (b). The α-Co_5Ge_3 has a Co_2Si-type orthorhombic structure with the space group *Pnma*. Three cobalt atoms form a triangular lattice with different length of Co-bonds and two nonequivalent cobalt sites Co1 and Co2 as illustrated in figures 1(a) and (b). Figure 1(c) shows the XRD pattern of an α-Co_5Ge_3 single crystal with its photo shown in the inset. Only (h00) Bragg peaks are presented, indicating that the exposed surface is *bc* plane. The *a* axis lattice parameter is estimated to be 0.4995 nm by using Bragg's law, which is consistent with the previous reported value [39]. The chemical composition of α-Co_5Ge_3 single crystals with the atomic ratio of Co:Ge $\approx$ 4.88:3 is identified by using EDX spectroscopy (table S1 in supplementary material (stacks.iop.org/JPhysCM/32/155802/mmedia)). This indicates that the samples contain non-negligible defects at Co sites, which may cause strong disorder in both lattice and spin structure.

To study the magnetic properties of α-Co_5Ge_3, temperature dependence of susceptibility χ ($\equiv$M/H) with field along both *a* axis ($H\|\ a$) and *bc* plane ($H\|\ bc$) are measured at indicated fields in the temperature range of 2 K–300 K, as shown in figures 2(a) and (b). The $\chi(T)$ curves are measured under sequences of zero-field-cooling (ZFC) and field-cooling (FC) at 0.02 T, 0.1 T and 1 T, respectively. FM transitions are observed with decreasing temperature under field applied along both directions. The FM transition temperatures T_c are determined by the dχ/d T curves at 0.02 T, with $T_c = 46$ K for $H\|\ a$ (χ_a) and $T_c = 50$ K for $H\|\ bc$ (χ_{bc}), respectively, which are consistent with the previous reported value of 46.4 K determined on polycrystalline samples [38].

Magnetization $M(H)$ isotherms are measured at different temperatures between 2 K and 300 K for $H \parallel a$ (M_a) and $H \parallel bc$ (M_{bc}), and shown in figures 2(c) and (d), respectively. According to the formula $\mu_0 H_{\rm eff} = \mu_0(H - N_d M)$, where N_d is the demagnetization factor, the effective magnetic field can be obtained. The value of N_d was calculated by using the method described in the literature [40]. In our case, however, the demagnetization is negligible due to the small value of M. The influence of demagnetization is thus not considered in following discussions. No saturation is reached in $M(H)$ isotherms up to 7 T below T_c. Similar behavior was observed in IFM $Zr(Mn,Fe)_2Zn_{20}$ with geometrical frustration [29], and thus indicates the existence of strong disorder in our samples. The inset of figure 2(b) displays the magnetic anisotropic ratio χ_a/χ_{bc} as a function of temperature at indicated magnetic field. At low field, χ_a is larger than χ_{bc}, indicating *a* axis is the easy axis of FM state. With the increase of the field, the anisotropic ratio decreases and is close to 1 at the field of 1 T. In figures 2(c) and (d), a lower critical field is extracted from M versus H curves with $H \parallel a$, comfirming that *a* axis is the easy axis.

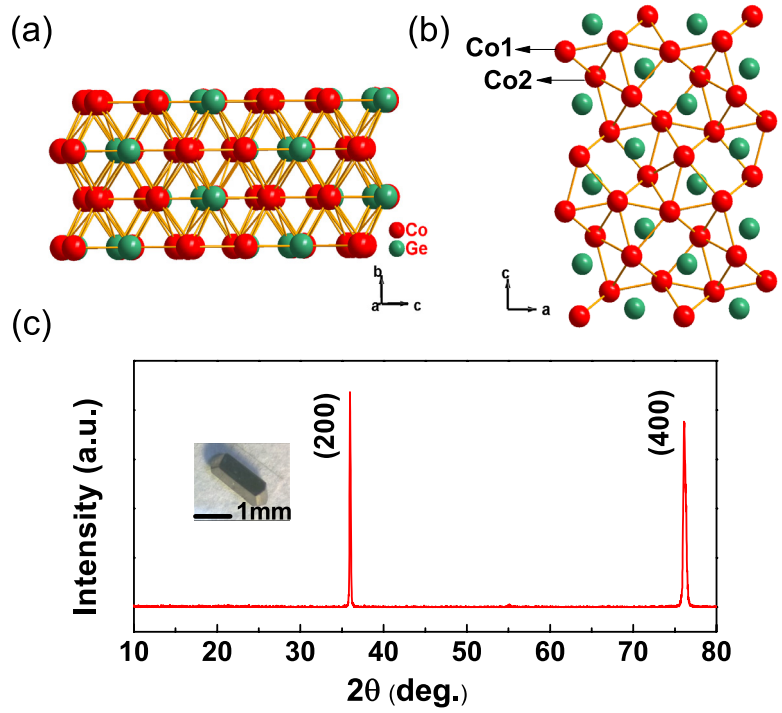

Figure 1. (a) The crystal structure of α-Co_5Ge_3 with the space group *Pnma*. (b) Quasi-two-dimensional triangular lattice network formed by Co atoms. (c) X-ray diffraction pattern of an α-Co_5Ge_3 single crystal. Inset shows a photo of a typical α-Co_5Ge_3 single crystal of 1 mm in length.

In the paramagnetic (PM) regime approximately 100 K–300 K, the susceptibility $\chi(T)$ can be fitted by the modified Curie–Weiss law,

$$\chi(T) = \chi_0 + \frac{C}{T - \theta_p} \tag{1}$$

where χ_0 is a temperature independent contribution, C is Curie constant related to the effective moment in the common manner and θ_p is the Weiss temperature [41]. The fitting parameters of χ_0, C, θ_p, and FM transition temperature T_c are extracted and summarized in the table 1. The $\theta_p^a = 67.0$ K and $C = 0.30$ emu K mol^{-1} for χ_a and $\theta_p^{bc} = 67.0$ K and $C = 0.32$ emu K mol^{-1} for χ_{bc}. The effective magnetic moment $\mu_{\rm eff}$ extracted from the fitting parameters is around 0.70 $\mu_{\rm B}$/Co for both χ_a and χ_{bc} using the formula $\mu_{\rm eff} = \sqrt{8C/5}$ [42].

According to the effective moment $\mu_{\rm eff}$, the number of magnetic carriers in the PM state q_c can be obtained experimentally from the local moment scenario [43],

$$\mu_{\rm eff}^2 = q_c(q_c + 2)\mu_{\rm B}^2. \tag{2}$$

Similarly, the number of magnetic carriers in the ordered state q_s below T_c can be determined from the saturated magnetic moment $\mu_{\rm sat}$ at low temperatures and high fields [43],

$$\mu_{\rm sat} = 2q_s\mu_{\rm B}. \tag{3}$$

In this work, from equations (2) and (3), $q_c = 0.22$ and $q_s = 0.035$ could be obtained with $\mu_{\rm eff} = 0.70\mu_{\rm B}$/Co and $\mu_{\rm sat} = 0.07$ $\mu_{\rm B}$/Co, determined from the M versus H curve at 2 K and 7 T. In our samples, this small value of saturated magnetic moment may come from the disorder induced by cobalt defects. Comparable values of saturated magnetic moment are observed in other IFMs, for instance 0.075 $\mu_{\rm B}$/Ni in Ni_3Al [44] and 0.16 $\mu_{\rm B}$/Zr in $ZrZn_2$ [45]. While the values in MnSi (0.4 $\mu_{\rm B}$/Mn) [46] and CoS_2 (0.84 $\mu_{\rm B}$/Co) [47] are much larger than what we observed in α-Co_5Ge_3. This difference is caused by various strength of magnetic correlations, spin fluctuation and disorder in these IFMs. The Rhodes–Wohlfarth (RW) ratio q_c/q_s of 6.3 is obtained, which indicates that α-Co_5Ge_3 is suitable for discussion under the itinerant electron model of ferromagnetism [48]. Then, both strong disorder and spin fluctuations could suppress the saturated magnetic moment $\mu_{\rm sat}$, and cause a large RW ratio. Of course, the low effective magnetic moment value above T_c also demonstrates the existence of itinerant electron ferromagnetism in α-Co_5Ge_3.

The $\chi(T)$ curve below T_c is analysed by using theoretical models of IFM. As shown in the inset of figure 2(a), below T_c, the FC $\chi(T)$ curve at 0.02 T deviates from the fitting curves of Stoner model (4) or spin fluctuation model (5), separately [49].

$$M(T) = M_0(1 - \frac{T^2}{T_c^2})^{\frac{1}{2}} \tag{4}$$

$$M(T) = M_0(1 - \frac{T}{T_c})^{\frac{1}{2}}. \tag{5}$$

While the experimental curve can be represented well by a combination of these two models, which indicates that both spin fluctuations and band split are important in α-Co_5Ge_3. Thus, the anisotropic T_c could be explained by spin fluctuations dominant along a axis, while correspondingly weak in bc plane [50].

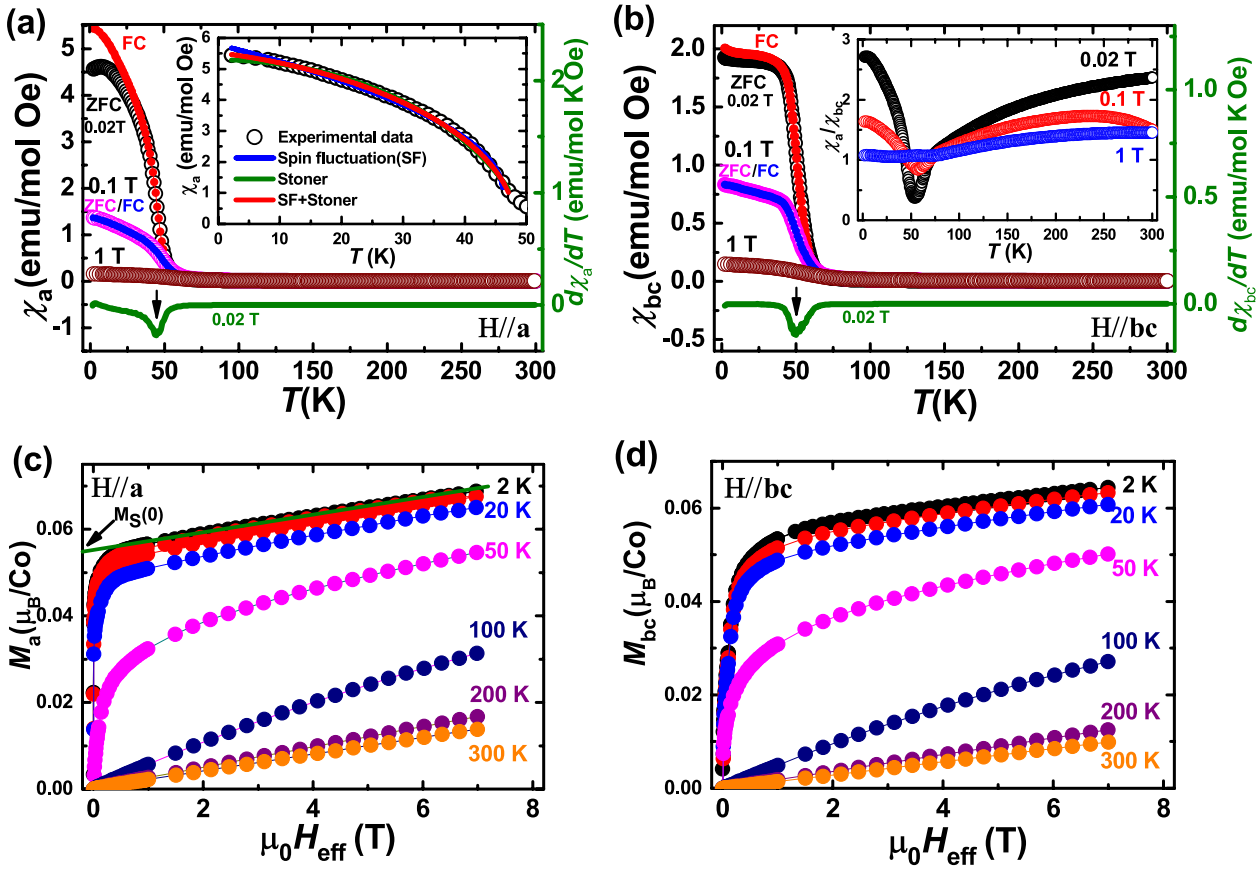

Figure 2. (a) Magnetic susceptibility χ and dχ/d T versus temperature for 2 K $\leqslant T \leqslant$ 300 K at the indicated magnetic fields applied along the a axis (χ_a, $H \| a$). Inset: below ferromagnetic transition temperature (T_c), χ versus T is fitted by the models of spin fluctuation, Stoner and a combination of both of them. (b) Magnetic susceptibility χ and dχ/d T versus temperature for 2 K $\leqslant T \leqslant$ 300 K at the indicated magnetic fields applied in the bc plane (χ_{bc}, $H \| bc$). Inset shows the magnetic anisotropic ratio of χ_a/χ_{bc} versus temperature at 0.02 T, 0.1 T and 1 T. (c) Isothermal magnetization M as a function of effective magnetic field at indicated temperatures with $H \| a$ axis (M_a); and (d) $H \| bc$ plane (M_{bc}). The intercept of green straight line is used to obtain the value of $M_s(0)$ in figure (c).

Table 1. FM transition temperatures are obtained from dχ/ dT and the three parameters χ_0, C and θ_p are obtained from fitting of the 1/($\chi - \chi_0$) versus T for α-Co_5Ge_3 single crystal by the modified Curie–Weiss Law.

Field direction	T_c (K)	Fit T range (K)	χ_0 (emu mol^{-1})	C (emu K mol^{-1})	θ_p (K)	μ_{eff} (μ_B/Co)	μ_{sat} (μ_B/Co)
$H \| a$	46	$100 \leqslant T \leqslant 300$	8.2×10^{-3}	0.30	67.0	0.69(3)	0.070
$H \| bc$	50	$100 \leqslant T \leqslant 300$	2.6×10^{-3}	0.32	67.0	0.71(5)	0.064

A bifurcation between ZFC and FC appears below T_c for $\chi(T)$ curves with 0.02 T field along both directions (see figures 2(a) and (b)). Similar behavior has been observed in anisotropic ferromagnetic compounds [51] or spin-disordered systems, such as spin-glass or ferromagnetic cluster glass compounds [3, 52]. The random defects at cobalt sites can be the origin of the spin-disordered state because the cobalt content is less than the stoichiometric number in 5. The disappearance of hysteresis at the field above 0.1 T suggests that this spin-disordered phase can be suppressed with increasing external magnetic field.

The ac susceptibility is employed to study the magnetic properties of α-Co_5Ge_3 below T_c. The real part of ac susceptibility is plotted in figures 3(a) and (b) as a function of temperature in the range from 2 K to 70 K. All curves in figures 3(a) and (b) show peaks at around 46 K independing on the frequency, which is consistent with the ferromagnetic transition temperature in dc susceptibility. Below 30 K, a broad hump appears in ac susceptibility with oscillated ac field along both a axis and bc plane. This broad hump implies that the low temperature magnetic phase develops with decreasing temperature and shows a characteristic of dynamic short range magnetic order. In order to clarify the frequency dependence of ac susceptibility at low temperature, the expanded views of ac susceptibility increments extracted by subtracting the FM background guided by the green solid lines(see figures 3(a) and (b)) are shown in figures 3(c) and (d), respectively. A peak was observed around 8 K in ac susceptibility along both directions. The temperatures of the peak position measured at different frequencies are denoted by T_f and represented by orange solid lines in figures 3(c) and (d). As shown in figure 3(c), T_f shifts monotonously to high temperature with increasing frequency

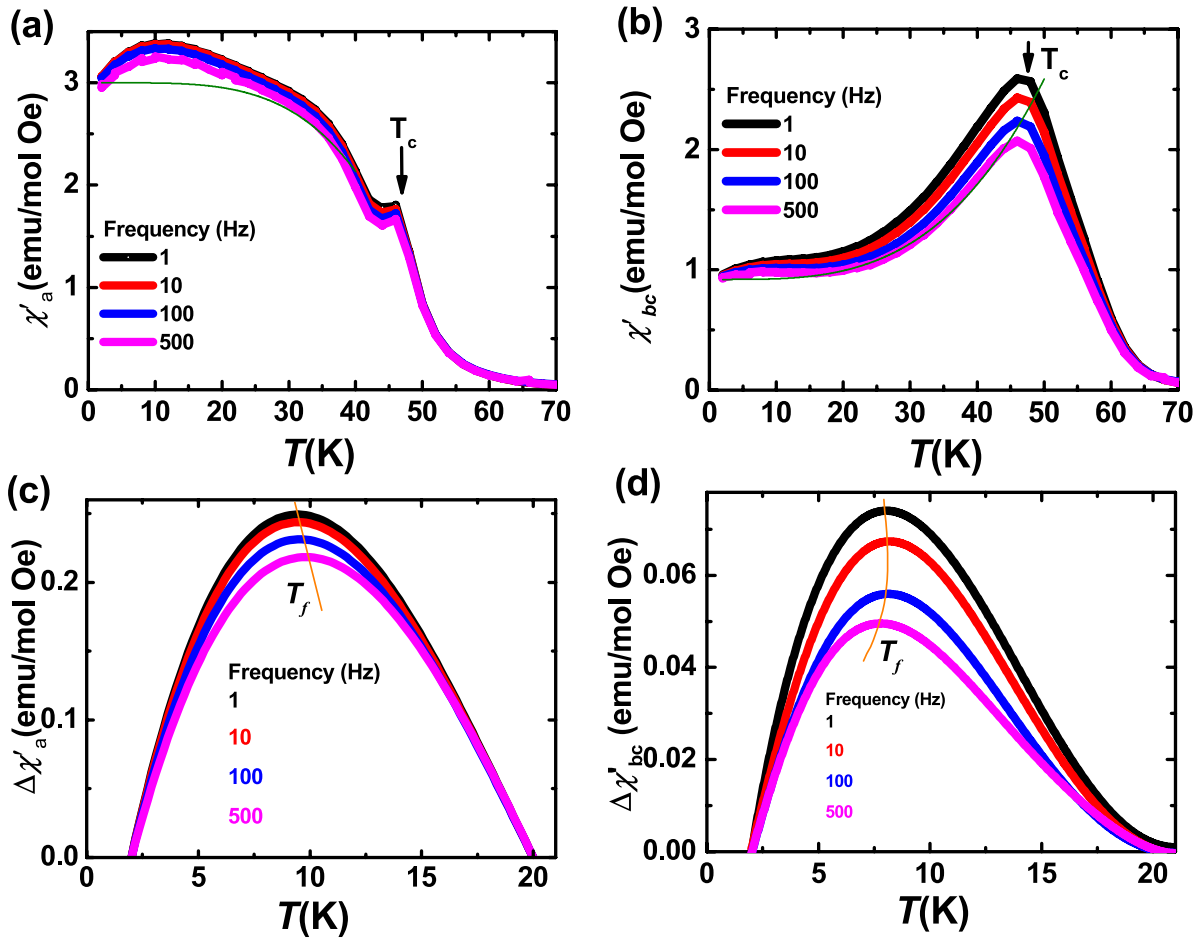

Figure 3. (a) Real part of ac susceptibility components versus temperature for 2 K $\leqslant T \leqslant$ 70 K measured at 1, 10, 100 and 500 Hz under zero dc field. Oscillated ac field of 10 Oe is applied along *a* axis; and (b) in the *bc* plane. The solid green lines in figures 2(a) and (b) represent the background of ferromagnetic transition. (c) The expanded views of low temperature ac susceptibility increments at 1, 10, 100 and 500 Hz with oscillated ac field of 10 Oe along *a* axis; and (d) in the *bc* plane. The solid orange lines in (c) and (d) denote the peak positions.

for $H \parallel a$. In contrast, T_f shifts non-monotonously with the increasing frequency and to a lower temperature with the frequency of 500 HZ for $H \parallel bc$. The different frequency dependence of T_f indicates that this low temperature magnetic phase is anisotropic. The shifting of T_f is often observed in spin glass or cluster glass systems, indicating that the low temperature magnetic phase is disordered. Similar spin glass states have been studied in some Ce-based heavy fermion systems, in which random site distributions of nonmagnetic/magnetic atoms (disorders) play a crucial role for the formation of spin-glass states [53–55]. In our samples, this spin-glass-like state is coexistent with long range ferromagnetic state, which may indicate a simple Co–Co magnetic interaction and eliminate the possibility of random site distribution of Co and Ge. Thus, the disorder induced by cobalt defects and spin fluctuations should be more likely responsible for the magnetic properties observed in α-Co_5Ge_3. Certainly, it is necessary and important to understand the nature of disorder in α-Co_5Ge_3 by using micro-structure analysis in future.

From the foregoing magnetic properties, α-Co_5Ge_3 is an IFM with spin fluctuations and non-negligible disorder, which is induced by cobalt defects. Therefore, this material provides an ideal platform to study the interplay between spin fluctuations and intrinsic disorder in IFMs. The transport properties have also been studied to explore the novel behaviors in this compound.

Figure 4(a) represents the temperature dependence of the electrical resistivity $\rho_{bc}(T)$ of α-Co_5Ge_3 single crystals measured at zero magnetic field, exhibiting a metallic behavior. A sharp peak of $d\rho_{bc}(T)/dT$ curve at 43 K, which is in good agreement with the T_c extracted from χ versus T curves in figure 2(a), is attributed to the FM transition. In figure 4(a), the fitting parameters of $\alpha = 3/2$, $\rho_0 = 0.098$ mΩ cm and $A = 0.237$ $\mu\Omega$ cm $K^{-1.5}$ are obtained from a power law fit of resistivity with the formula of $\rho_{bc} = \rho_0 + AT^{\alpha}$ in the range from 1.6 K and 30 K. A same power law behavior has been observed in FM phases of IFMs Ni_3Al and YNi_3 [17], metallic glass phases of HF systems [3], and dirty(disordered) HF metals near an antiferromagnetic quantum critical point [56]. It is also consistent with some theoretical predictions [3, 34, 57]. The effect of spin fluctuations and disorder could change scattering process of the conduction electrons and lead to the emergence of NFL behavior. Above T_c, T-sublinear resistivity behavior is different from the resistivity of conventional magnetic metals with localized spins [58] and is also observed in ferromagnetic metals with strong spin fluctuations [59, 60].

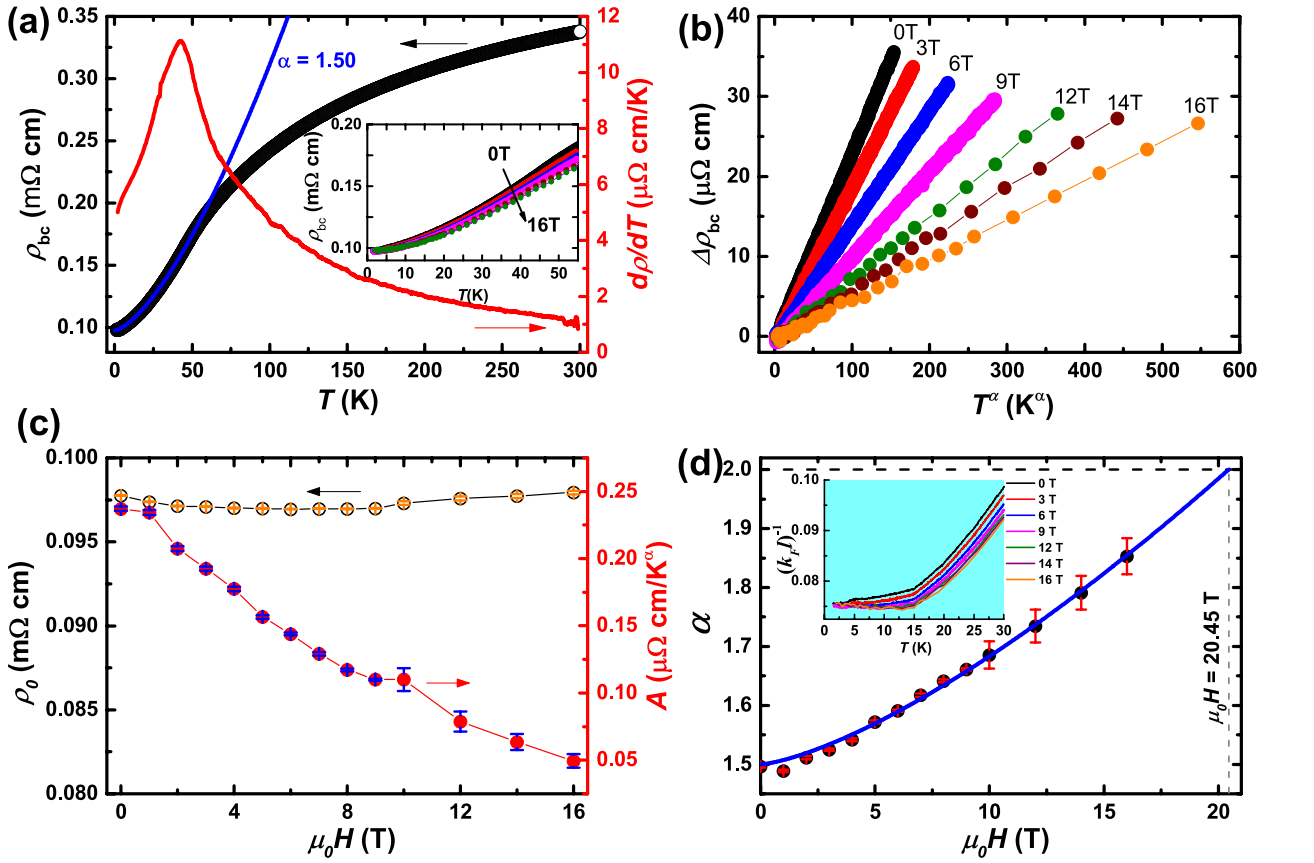

Figure 4. (a) Temperature dependence of in − plane resistivity $\rho_{bc}(T)$ and its derivative ($d\rho_{bc}$/ dT) at the temperature range from 1.6 K to 300 K under zero field. Blue solid line: using $\rho_{bc}(T) = \rho_0 + AT^{\alpha}$ fit the resistivity measured below 30 K, $\alpha = 1.50$. Inset: temperature dependence of $\rho_{bc}(T)$ at different field from 0 to 16 Tesla and in the temperature range from 1.6 K to 55 K. (b) $\Delta\rho_{bc} = \rho_{bc} - \rho_0$ as a function of T^{α} at indicated magnetic field, where $\alpha = \partial \ln(\rho(T) - \rho_0)/\partial \ln T$ is the power law exponent at each field. (c) Power law behavior coefficients of ρ_0 and A as a function of applied field. (d) Magnetic field dependence of the power law exponent α, corresponding to the $\rho_{bc}(T)$ in (a) under magnetic field up to 16 T. The solid blue line is the fit of experimental data with a power function. Inset: temperature dependence of $(k_F l)^{-1}$ at indicated fields in the temperature range from 1.6 K to 30 K.

Temperature dependence of in-plane resistivity at indicated magnetic fields show metallic behavior and decrease with increasing field (see inset of figure 4(a)).

$\Delta\rho_{bc} = \rho_{bc} - \rho_0$ on a scale of T^{α} up to 30 K under indicated magnetic fields, as shown in figure 4(b), present a linear dependence, indicating a good power law fitting below 30 K. Figure 4(c) displays the evolution of power law fitting coefficients ρ_0 and A of resistivity as a function of applied field. The value of ρ_0 is field independent and equals to 0.097 mΩ cm. Whereas, the value of A decreases with the increasing field. The coefficient A means the quasiparticle interaction, more precisely the renorma1ization of the quasiparticles masses at the Fermi surface, corresponding to the density of states at the Fermi level [61, 62]. The change of A represents the evolution of Fermi surface with changing magnetic field.

The magnetic field dependence of power law exponent α are shown in figure 4(d). The value of α increases with the increasing field and reaches 1.85 at 16 T. According to the previous theoretical prediction [33], the resistivity ρ(T) crosses over from a FL T^2 behavior to a NFL $T^{\alpha(W)}$ behavior with the presence of disorder and fluctuations, where W is indicating the strength of disorder and the exponent, α, is found to be dependent on W. Here, W can be estimated from the Ioffe–Regel parameter $k_F l$, with $W \approx (k_F l)^{-1}$ [34]. The value of $k_F l$ could be calculated by using the formula $k_F l = \{(3\pi^2)^{2/3}\hbar[R_H(T)]^{1/3}\}/[\rho(T)e^{5/3}]$ [63]. In this work, $k_F l$ is calculated using the corresponding values of R_0 (R_H) (see figure 6(c)) and ρ(T) (see figure 4(a)). The inset of figure 4(d) plots the evolution of $(k_F l)^{-1}$ as a function of temperature at indicated fields, which indicates that W is sensitive to applied field due to the suppression of spin disorder. Consequently, $\alpha(W)$ is expected to be a function of magnetic field, with a power function relation $\alpha(W) \sim H^{\gamma}$ [57, 64]. In figure 4(d), α variation can be well fitted by a power function, and the α value may attain 2 with $\mu_0 H = 20.45$ T in this trend. A high enough external magnetic field could suppress the disorder and spin fluctuations, and restore the FL behavior in the resistivity below 30 K.

Magnetic field dependence of in-plane magnetoresistance (MR) at indicated temperatures with $H \parallel a$ are shown in figures 5(a) and (b), in which MR is calculated by $\Delta\rho_{bc}/\rho_{bc} = [\rho_{bc}(\mu_0 H) - \rho_{bc}(0)]/\rho_{bc}(0)$. The negative MR is presented under the magnetic field up to 9 T at different temperatures. To clarify the evolution of MR versus T, the |MR| ratios at 9 T as a function of temperature are shown in figure 5(c). The absolute value of MR increases with increasing temperature in the FM

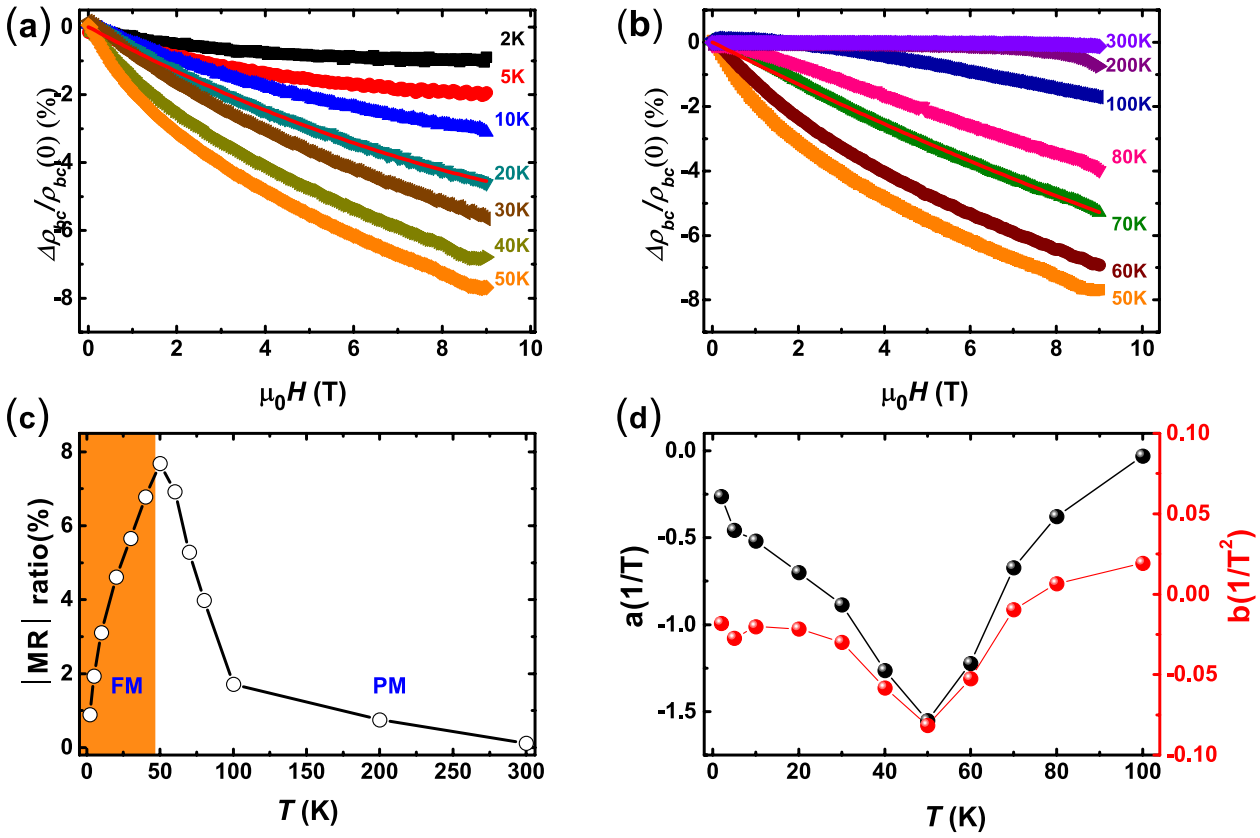

Figure 5. (a) Magnetoresistance with $H \parallel a$ at 2 K–50 K, and (b) at 50 K–300 K. The red solid lines in (a) and (b) are the fitting curves of MR at 20 K and 70 K, respectively, representing typical examples of the goodness of fit. (c) The temperature dependence of the |MR| ratio $|(\rho_{bc}(9\ \mathrm{T}) - \rho_{bc}(0))/\rho_{bc}(0)|$. (d) The evolution value of fitting parameters extracted from the MR fitting results by using the relation MR $\propto a\ H - b\ H^2$. FM: ferromagnetic region; PM: paramagnetic region.

region and reaches the maximum value ($\sim$8%) at 50 K (near the T_c) due to the strong suppression of electron-spin scattering, then followed by a decrease. Upon further increasing temperature to 300 K, the absolute value of MR decreases and reaches zero at room temperature. The field dependence of MR can be fitted by the relation MR $\propto a\ H - b\ H^2$ at the temperature from 2 K to 100 K [65]. Two of fitting curves for T = 20 K and 70 K are selected and presented in figures 5(a) and (b), respectively. For itinerant electron systems, the effect of dynamics spin fluctuations is more significant than that of spin waves [43], for example, spin fluctuations play a dominate role in itinerant ferromagnet metals Sc_3In and Ni_3Al [61, 66]. The well fitting results in α-Co_5Ge_3, in particular at temperature lower than T_c, reveal that spin fluctuations not only play an important role around T_c, but also have predominant effect at $T \ll T_c$. Temperature dependence of coefficients a and b are summarized in figure 5(d). The maximum values of both a and b are obtained at 50 K, which approaches to the magnetic transition temperature. This indicates that the spin fluctuations are strongest at 50 K, which directly leads to the maxmium negative magnetoresistance.

To elucidate the physical properties in α-Co_5Ge_3 further, the magnetic field dependence of Hall resistivity ρ_{xy} at different temperatures under $H \parallel a$ are examined and shown in figures 6(a) and (b). In general, the total Hall resistivity ρ_{xy} in ferromagnetic conductors comprises two terms [67],

$$\rho_{xy} = R_0\mu_0 H + R_s M, \tag{6}$$

where R_0 and R_s represent the ordinary (Lorentz-force) and anomalous Hall coefficients, respectively. ρ_{xy} increases linearly with the increase of magnetic field at temperature above 100 K, while shows non-linear dependence between 50 K and 80 K. When the temperature decreases below T_c of 46 K, both ordinary Hall effect and anomalous Hall effect make contribution to ρ_{xy} [68]. The values of R_0 and R_s in the empirical formula equation (4) obtained mainly in the linear region of high magnetic field of $\rho_{xy}(H)$ curves, which is guided by black fitted line at 50 K in figure 6(a), are displayed in figures 6(c) and (d), respectively. The slope and y-axis intercept (figure 6(a)) are corresponding to the R_0 and ρ_{xy}^A, respectively. The value of R_s can be determined by using the formula $\rho_{xy}^A = R_s\ M_s$, with the M_s value obtained from $M(H)$ curves in figure 2(c) [69]. The temperature dependence of R_0 is shown in figure 6(c). R_0 reaches the maximum value of 3.8×10^{-10} $\mathrm{m^3C^{-1}}$ at 100 K and changes sign around 50 K, implying that the dominant carrier changes from electron to hole with increasing temperature. The sign change of R_0 also indicates that the α-Co_5Ge_3 has a multiple-band electronic structure. And this evolution of the Fermi surface with changing temperature around T_c can be attributed to the magnetic phase transition. The R_s presented in figure 6(d), which is about two orders of magnitude larger than that of the conventional itinerant ferromagnets, such as

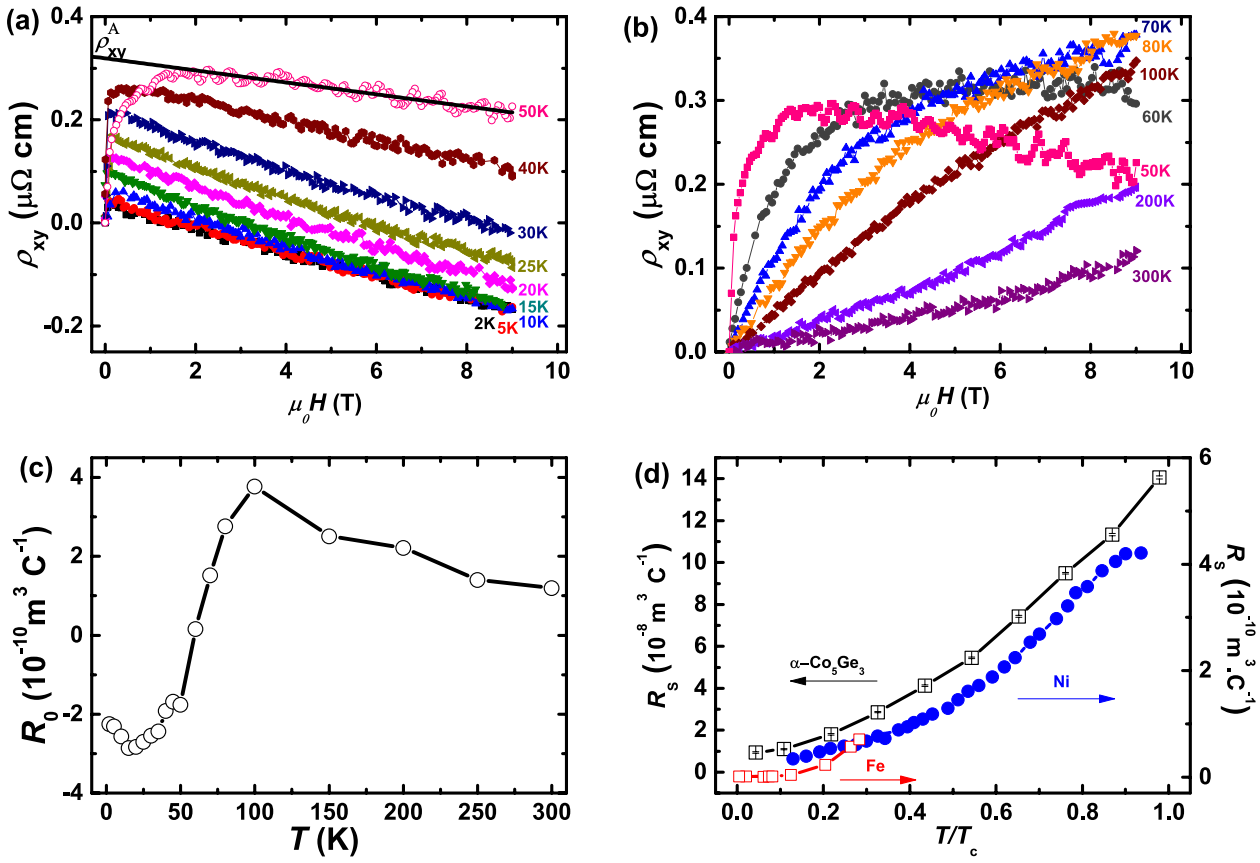

Figure 6. Magnetic field dependence of the Hall resistivity ρ_{xy} at (a) 2 K–50 K and (b) 50 K–100 K. The black solid line in panel (a) represents the linear fitting of $\rho_{xy}(H)$ in the high magnetic field region at $T = 50$ K. (c) Temperature dependence of the ordinary Hall coefficient of R_0. (d) Anomalous Hall coefficient R_s as a function of the reduced temperature (T/T_c) for α-Co_5Ge_3, pure Fe and Ni [70, 71].

Fe and Ni [70, 71], is positive and increases with increasing temperature below T_c. As T/T_c approach to 0, the residual component of R_s reaches 0.85×10^{-8} m^{3}C^{-1}, which indicates that spin disorder has a little contribution to R_s at zero temperature. At T_c, the value of R_s reaches the 1.40×10^{-7} m^3 C^{-1} which is comparable to the R_s value in IFM metal Fe_3Sn_2 with geometrical frustration [72, 80], supporting the existence of strong disorder in α-Co_5Ge_3.

In order to understand the mechanism of anomalous Hall effect (AHE) in α-Co_5Ge_3, the log–log plot of ρ_{xy}^{A} versus logρ_{xx} (Here ρ_{bc} is represented as ρ_{xx}.) is shown in figure 7(a). The magenta and cyan solid lines show the fitting results using the formula $\rho_{xy}^{A} \propto \rho_{xx}^{\beta}$. At the temperature of 30 K–50 K, the slope β of fitting line is estimated to be ~2.0 indicating the existence of intrinsic KL mechanism [73] or extrinsic side-jump mechanism [68]. In the T range from 2 K to 25 K, β has an intriguing exponent value 6.9, which cannot be explained by conventional mechanisms. This temperature range is in line with that displaying NFL behavior, indicating that strong disorder play a dominant role in determining the transport properties. The large β value was observed in heterogeneous ferromagnetic systems, such as $\beta = 3.1$ in Fe/Cr mutlilayers [74], $\beta = 3.7$ in Co–Ag granular films [75], $\beta = 5.7$ in Co/Pd multilayers [76], even an unexpected high exponent $\beta = 17.6$ in ε–Fe_3N nanocrystalline films [77]. A large $\beta = 3.7$ was also observed in polycrystalline Fe_3Sn_2 [78], which is larger than $\beta = 2$ observed in homogeneous Fe_3Sn_2 single crystals [80]. The reason leading to such large β value in magnetic mutlilayers films or polycrystalline sample is that the mean-free path of carrier is larger or comparable than the layer thickness or grain size, respectively [79, 80]. These results indicate that disorder may give rise to large β value. The effective mean free path λ_{eff} in α-Co_5Ge_3 is estimated using the Drude–Sommerfeld formula $\rho_{xx} = m^* v_F/ne^2\lambda_{\text{eff}}$, in which carrier concentration $n_H = 1/eR_0$ and Fermi velocity $v_F = \hbar\sqrt[3]{3\pi^2 n}/m^*$. Thus λ_{eff} can be obtained from experimental values of carrier concentration n and ρ_{xx} [75], which ranges from 12.5 Å to 14.7 Å in our samples below 30 K. The value of λ_{eff} may be larger or comparable to the characteristic size of spin-disordered phase in α-Co_5Ge_3, resulting in a large exponent $\beta = 6.9$. This strong disorder observed in our samples could arise from cobalt defects and/or spin frustrations. To clarify the contribution from each factor, further experiments on stoichiometric α-Co_5Ge_3 are needed.

Figure 7(b) is the plot of the total Hall conductivity σ_{xy} ($=\rho_{xy}/(\rho_{xx}^2 + \rho_{xy}^2)$) versus $\mu_0 H$ at indicated temperatures below 50 K. σ_{xy} curves have no hysteresis loops, which is consistent with M versus H plots in figure 2. Figure 7(c) shows the T dependence of σ_{xy}^{A} ($=\rho_{xy}^{A}/(\rho_{xx}^2 + \rho_{xy}^{A})$) and magnetization M measured at 1 T from 2 to 50 K. At the temperature of 30 K–50 K, σ_{xy}^{A} is T independent and approximately equal to 11.8 S cm^{-1}. M

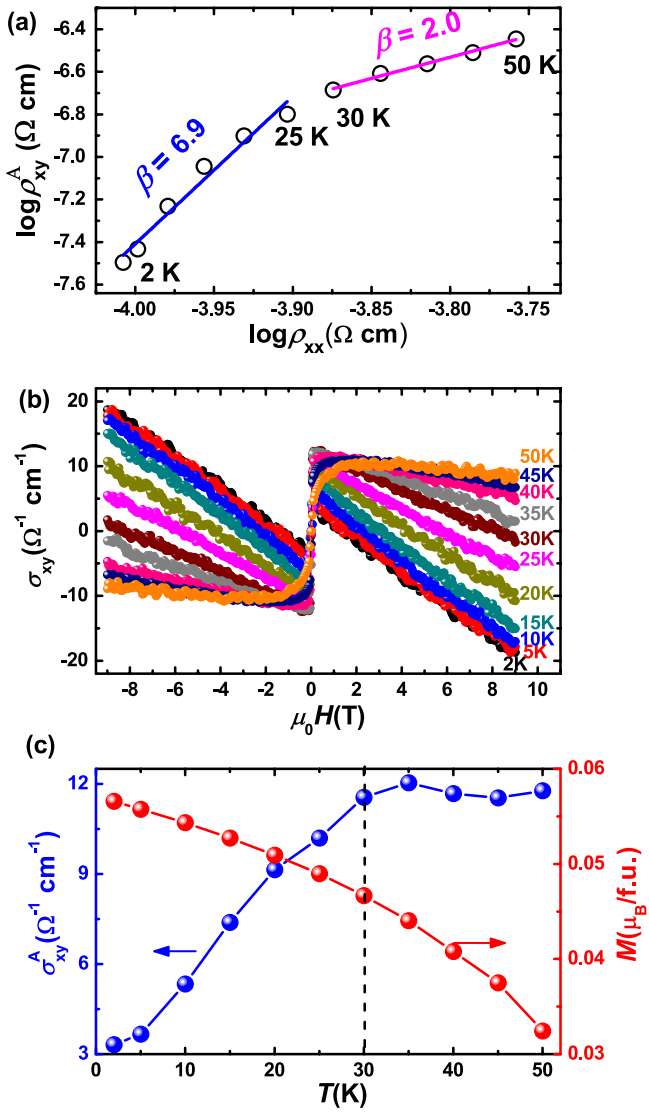

Figure 7. (a) Plot of logρ^A_{xy} versus logρ_{xx}. The magenta and cyan solid lines are the fits using the relation $\rho^A_{xy} \propto \rho^\beta_{xx}$ below and above 30 K, respectively. (b) σ_{xy} (obtained from curves ρ_{xy} and ρ_{xx}) versus $\mu_0 H$ at indicated temperatures. (c) Temperature dependence of σ^A_{xy} and magnetization M.

versus T, however, has an obvious temperature dependence in this temperature range. Therefore, σ^A_{xy} is not proportional to M, ruling out KL mechanism in this region [81]. Thus, AHE at 30 K–50 K is dominated by side-jump mechanism. According to the above discussions, the rapid decrease of σ^A_{xy} below 30 K, should be caused by the strong disorder and could not be explained by conventional mechanisms.

4. Conclusions

In summary, α-Co_5Ge_3 is an itinerant FM with FM transitions at $T_c = 45$ K for $H \parallel a$ and $T_c = 50$ K for $H \parallel bc$, respectively. Unsaturated magnetization and large RW ratio suggest that the existence of strong disorder arising from cobalt defects and spin fluctuations. The ac susceptibility also reveals that the existence of spin glass phase below 30 K due to the strong disorder. A NFL behavior with the form of $\rho_{bc} = \rho_0 + AT^\alpha$ ($1.50 \leqslant \alpha \leqslant 1.85$) is observed in temperature dependence of resistivity and attributed to disorder induced by cobalt defects and spin fluctuations. The increase of exponent α with applied magnetic field is attributed to the suppression of spin fluctuations and disorder under external field. The Hall resistivity show a sign change of ordinary Hall coefficient R_0 around 50 K, indicating the multiple-band electronic structure and the change of Fermi surface induced by FM phase transition. Below 30 K, the large exponent $\beta \sim 6.9$ extracted from σ^A_{xy} versus σ_{xx} plot indicates that the strong disorder play an important role on the transport properties. Our results reveal the coexistence of spin fluctuations and disorder in α-Co_5Ge_3, which makes it an ideal platform to study the interplay of disorder and spin fluctuations.

Acknowledgments

This work is supported by the National Key Research and Development Program of China (Grant No. 2016YFA0300404 and No. 2017YFA0402900) and the NSFC (Grants No. U1432138, No. 11474288, No. 11574317, Grant No. 11574322 and No. U1732276). YX thanks the support of the Hundred Talents Program of the Chinese Academy of Sciences. A portion of this work was supported by the High Magnetic Field Laboratory of Anhui Province.

ORCID iDs

Meng Song https://orcid.org/0000-0001-6864-5292
Cong Xian https://orcid.org/0000-0001-5436-8220
Jiangpeng Song https://orcid.org/0000-0001-5435-5251
Lei Zhang https://orcid.org/0000-0001-5427-6561

References

[1] Cox D L 1987 *Phys. Rev. Lett.* **59** 1240
[2] Stewart G R 2001 *Rev. Mod. Phys.* **73** 797
[3] Miranda E and Dobrosavljević V 2005 *Rep. Prog. Phys.* **68** 2337
[4] Löhneysen H V, Rosch A, Vojta M and Wölfle P 2007 *Rev. Mod. Phys.* **79** 1015
[5] Lee S S 2018 *Annu. Rev. Condens. Matter Phys.* **9** 227–44
[6] Mathur N D, Grosche F M, Julian S R, Walker I R, Freye D M, Haselwimmer R K W and Lonzarich G G 1998 *Nature* **394** 39
[7] Gegenwart P, Si Q and Steglich F 2008 *Nat. Phys.* **4** 186
[8] Anderson P W 1997 *The Theory of Superconductivity in the High-Tc Cuprates* (Princeton, NJ: Princeton University Press)
[9] Orenstein J and Millis A J 2000 *Science* **288** 468
[10] Cooper R A *et al* 2009 *Science* **323** 603
[11] Analytis J G, Kuo H-H, McDonald R D, Wartenbe M, Rourke P M C, Hussey N E and Fisher I R 2014 *Nat. Phys.* **10** 194
[12] Kurosaki Y, Shimizu Y, Miyagawa K, Kanoda K and Saito G 2005 *Phys. Rev. Lett.* **95** 177001
[13] Soltanieh-ha M and Feiguin A E 2012 *Phys. Rev.* B **86** 205120
[14] Furukawa T, Kobashi K, Kurosaki Y, Miyagawa K and Kanoda K 2018 *Nat. Commun.* **9** 307

[15] Svanidze E *et al* 2015 *Phys. Rev.* X **5** 011026
[16] Nicklas M, Brando M, Knebel G, Mayr F, Trinkl W and Loidl A 1999 *Phys. Rev. Lett.* **82** 4268
[17] Steiner M J, Beckers F, Niklowitz P G and Lonzarich G G 2003 *Physica* B **329–33** 1079
[18] Hertz J A 1976 *Phys. Rev.* B **14** 1165
[19] Millis A J 1993 *Phys. Rev.* B **48** 7183
[20] Zülicke U and Millis A J 1995 *Phys. Rev.* B **51** 8996
[21] Uhlarz M, Pfleiderer C and Hayden S M 2004 *Phys. Rev. Lett.* **93** 256404
[22] Smith R P, Sutherland M, Lonzarich G G, Saxena S S, Kimura N, Takashima S, Nohara M and Takagi H 2008 *Nature* **455** 1220
[23] Miranda E, Dobrosavljević V and Kotliar G 1997 *Phys. Rev. Lett.* **78** 290
[24] Dobrosavljević V and Kotliar G 1997 *Phys. Rev. Lett.* **78** 3943
[25] Idzikowski B, Kudryavtsev Y V, Hyun Y H, Lee Y P and Klenke J 2006 *J. Alloys Compd.* **423** 267
[26] Sokolov D A, Aronson M C, Gannon W and Fisk Z 2006 *Phys. Rev. Lett.* **96** 116404
[27] Jia S, Budko S L, Samolyuk G D and Canfield P C 2007 *Nat. Phys.* **3** 334
[28] Okamoto Y, Shimizu T, Yamaura J, Kiuchi Y and Hiroi Z 2010 *J. Phys. Soc. Japan* **79** 093712
[29] Svanidze E, Kindy M II, Georgen C, Fulfer B, Lapidus S, Chan J and Morosan E 2016 *J. Magn. Magn. Mater.* **416** 401
[30] Sacépé C, Chapelier B, Baturina T I, Vinokur V M, Baklanov M R and Sanquer M 2008 *Phys. Rev. Lett.* **101** 157006
[31] Jia S, Ni N, Samolyuk G D, Safa-Sefat A, Dennis K, Ko H, Miller G J, Budko S L and Canfield P C 2008 *Phys. Rev.* B **77** 104408
[32] Patel N D, Mukherjee A, Kaushal N, Moreo A and Dagotto E 2017 *Phys. Rev. Lett.* **119** 086601
[33] Sen S, Vidhyadhiraja N S and Jarrell M 2018 *Phys. Rev.* B **98** 075112
[34] Rosch A 1999 *Phys. Rev. Lett.* **82** 4280
[35] MacLaughlin D E, Bernal O O, Heffner R H, Nieuwenhuys G J, Rose M S, Sonier J E, Andraka B, Chau R and Maple M B 2001 *Phys. Rev. Lett.* **87** 066402
[36] Antolak A, Oleszak D, Pekala M and Kulik T 2007 *Mater. Sci. Eng.* A **449** 440–3
[37] Malaman B, Steinmetz J and Roques B 1980 *J. Less-Common Met.* **75** 155
[38] Zhou G F and Bakker H 1993 *Phys. Rev.* B **48** 13383
[39] Panday P K and Schubert K 1969 *J. Less-Common Met.* **18** 175
[40] Aharoni A 1998 *J. Appl. Phys.* **83** 3432
[41] Smart J S 1966 *Effective Field Theories of Magnetism* (New York: Saunders)
[42] Anand V K, Dhaka R S, Lee Y, Harmon B N, Adam Kaminski and Johnston D C 2014 *Phys. Rev.* B **89** 214409
[43] Santiago J M, Huang C-L and Morosan E 2017 *J. Phys.: Condens. Matter* **29** 373002
[44] de Boer F R, Schinkel C J, Biesterbos J and Proost S 1969 *J. Appl. Phys.* **40** 1049
[45] Yelland E A, Yates S J C, Taylor O, Griffiths A, Hayden S M and Carrington A 2005 *Phys. Rev.* B **72** 184436
[46] Demishev S V *et al* 2012 *Phys. Rev.* B **85** 045131
[47] Adachi K, Sato K and Takeda M 1969 *J. Phys. Soc. Japan* **26** 631
[48] Rhodes P and Wohlfarth E P 1963 *Proc. R. Soc.* A **273** 247
[49] Mohn P 2003 *Magnetism in the Solid State, an Introduction* (Berlin: Springer)
[50] Adachi K, Matsui M and Fukuda Y 1980 *J. Phys. Soc. Japan* **48** 62
[51] Liu Y and Petrovic C 2018 *Phys. Rev.* B **97** 174418
[52] Mydosh J A 2015 *Rep. Prog. Phys.* **78** 052501
[53] Huo D, Sakurai J, Kuwai T and Isikawa Y 2001 *Phys. Rev.* B **64** 224405
[54] Nishioka T, Tabata Y, Taniguchi T and Miyako Y 2000 *J. Phys. Soc. Japan* **69** 1012
[55] Lebarski A S 2009 *J. Alloys Compd.* **480** 912
[56] Gegenwart P *et al* 1998 *Phys. Rev. Lett.* **81** 1501
[57] Arrachea L, Dalidovich D, Dobrosavljevic V and Rozenberg M J 2004 *Phys. Rev.* B **69** 064419
[58] Kasuya T 1956 *Prog. Theor. Phys.* **16** 58
[59] Adachi K *et al* 1979 *J. Phys. Soc. Japan* **46** 1474
[60] Fisher M E and Langer J S 1968 *Phys. Rev. Lett.* **20** 665
[61] Sasakura H, Suzuki K and Masuda Y 1984 *J. Phys. Soc. Japan* **53** 352
[62] Thessieu C, Flouquet J, Lapertot G, Stepanov A N and Jaccard D 1995 *Solid State Commun.* **95** 707
[63] Chand M *et al* 2009 *Phys. Rev.* B **80** 134514
[64] Sachdev S, Read N and Oppermann R 1995 *Phys. Rev.* B **52** 10286
[65] Kaul S N 2005 *J. Phys.: Condens. Matter* **17** 5595
[66] Masuda Y, Hioki T and Oota A 1977 *Physica* B **91** 291
[67] Hurd C M 2012 *The Hall Effect in Metals and Alloys* (Berlin: Springer)
[68] Nagaosa N, Sinova J, Onoda S, MacDonald A H and Ong N P 2010 *Rev. Mod. Phys.* **82** 1539
[69] Yan J *et al* 2017 *Appl. Phys. Lett.* **111** 022401
[70] Volkenshtein N V and Fedorov G V 1960 *Sov. Phys.—JETP* **11** 48
[71] Kaul S N 1979 *Phy. Rev.* B **20** 5122
[72] Ye L *et al* 2018 *Nature* **555** 638
[73] Karplus R and Luttinger J M 1954 *Phys. Rev.* **95** 1154
[74] Song S N, Sellers C and Ketterson J B 1991 *Appl. Phys. Lett.* **59** 479
[75] Xiong P, Xiao G, Wang J Q, Xiao J Q, Jiang J S and Chien C L 1992 *Phys. Rev. Lett.* **69** 3220
[76] Guo Z B, Mi W B, Aboljadayel R O, Zhang B, Zhang Q, Barba P G, Manchon A and Zhang X X 2012 *Phys. Rev.* B **86** 104433
[77] Cheng Y H, Zheng R K, Liu H, Tian Y and Li Z Q 2009 *Phys. Rev.* B **80** 174412
[78] Kida T, Fenner L A, Dee A A, Terasaki I, Hagiwara M and Wills A S 2011 *J. Phys.: Condens. Matter* **23** 112205
[79] Zhang S 1995 *Phys. Rev.* B **51** 3632
[80] Wang Q, Sun S, Zhang X, Pang F and Lei H 2016 *Phys. Rev.* B **94** 075135
[81] Onose Y and Tokura Y 2006 *Phys. Rev.* B **73** 174421